# Study of Optimal Behavior in Complex Virtual Training Systems

Jose San Martin

Universidad Rey Juan Carlos, Madrid
jose.sanmartin@urjc.es

**Abstract.** In previous works we have studied the behavior of simple training systems integrated by a haptic device basing on criteria derived from Manipulability concept. The study of complex systems needs to re-define the criteria of optimal design for these systems. It is necessary to analyze how the workspace of two different haptics, simultaneously on the same model, limits the movement of each other. Results of the new proposed measures are used on Insight ARTHRO VR training system. The Minimally Invasive Surgery (MIS) techniques use miniature cameras with microscopes, fiber-optic flashlights and high definition monitors. The camera and the instruments are inserted through small incisions on the skin called portals. The trainer uses two PHANToM OMNi haptic devices, one representing the camera and other the surgical instrumental.

**Keywords:** Haptics, Workspace Interference, Manipulability, Optimal Designing.

## 1 Introduction

When developing a VR simulation, on the one hand we are moving in the real world by manipulating a haptic device; this movement corresponds to a movement of an object in our simulation, that is, in the virtual environment. So we must first study the portion of space that can be achieved with our device, called the real workspace (RW). Therefore should be made according to his characterization of an efficiency measure based on the criterion of Manipulability [1], which will allow us to redefine the subareas we want to work from all the available area. So, according to the virtual environment to define, called virtual workspace (VW), this portion of the RW must be chosen.

The Minimally Invasive Surgery (MIS) techniques use miniature cameras with microscopes, tiny fiber-optic flashlights and high definition monitors. The camera and the instruments are inserted through small incisions on the skin. The visual control of organs and surgical instruments is done thanks to the image provided by the video camera [2][3]. These procedures are complex to perform and require specialized training in order to obtain proficiency in the skills [4]. Therefore this paper proposes a methodology to optimize the design of these training systems, so that depending on the surgical technique to implement, it is possible to define an optimal configuration of virtual training system for each case.

R. Shumaker (Ed.): Virtual and Mixed Reality, Part II, HCII 2011, LNCS 6774, pp. 64–72, 2011.

## 2 Manipulability Solid

Among several indices that allow us to study the quality of systems involving several haptic devices we have chosen the well known concept of Manipulability [5] [6] [7], since it allows a quantitative value to the quality of the system.

Manipulability of a device is its ability to move freely in all directions into the workspace [8]. In these terms the Manipulability for each device configuration, is a tool for evaluating the quality and the performance in the designing of a manipulator device [1] [9] [10].

From the original formulation of Yoshikawa, we use the formulation of Manipulability proposed by [11]:

$$\mu = \sigma_{min}(J_u)/\sigma_{max}(J_u) \quad (1)$$

Where:

$\sigma_{min}$ and $\sigma_{max}$ are the minimum and maximum singular values of $J_u$, upper half of the manipulator Jacobian matrix.

For each haptic we can define a volume as the Manipulability Solid associated to the device (fig. 1).

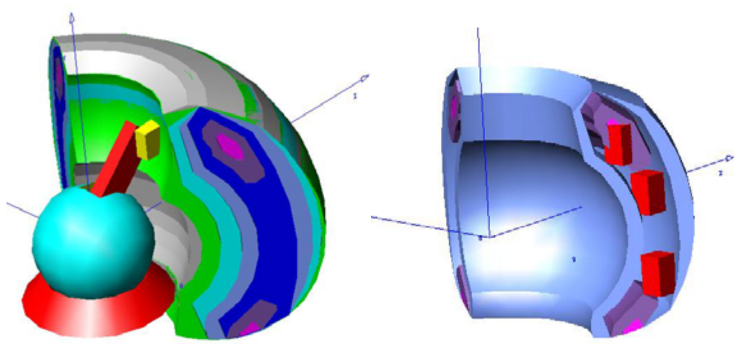

**Fig. 1.** 3D Solid of Manipulability (left). Detail of positioning options of a VW inside the RW (right).

From whole the RW a portion is selected: the virtual environment which we called Virtual Workspace (VW), in red in fig. 1-right. We place VW inside RW taking advantage of best zones according to Manipulability index (different options of positioning a VW are presented).

## 3 Useful Manipulability

During a simulation session we find that there are zones of VW where the specific task is effectuated. So it is desirable than the haptic device provides its best performance in these zones. For a specific task to be done, we define Navigation Frequency Map-NFM as the VW where we assign to each voxel the number of times is visited when doing this task.

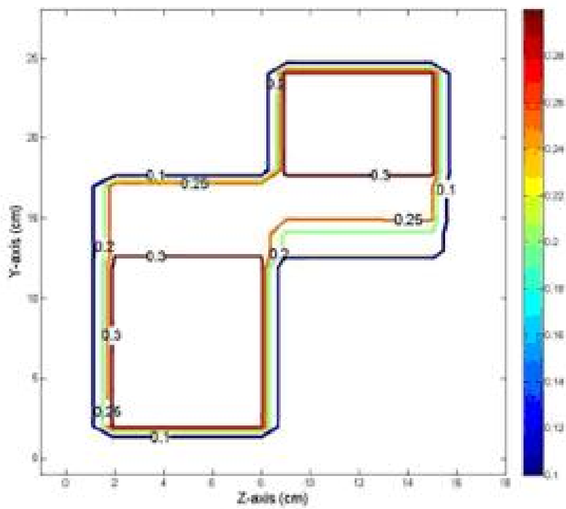

**Fig. 2.** 2D Portion of NFM-Diagnostic Arthroscopy. NFM is a 3D object in XYZ, figure represents a portion for an X defined value. Level curves represent frequency values in 10e-3.

We discretize RW in a grid of voxels so we call $\mu_{ijk}$ the value of manipulability calculated using (1) in each cell (i, j, k).

$$\hat{\mu}_v = \sum_{ijk} \mu_{vijk} \cdot f_{ijk} \tag{2}$$

where:

$\mu_{v\,ijk}$ is the distribution of Manipulability into a cell.

$f_{ijk}$ is the frequency of visits sampled during a simulation session in a cell.

Figure 2 shows an example of a NFM obtained from the simulation of a Diagnostic Arthroscopy.

## 4 A New Algorithm for Optimal Positioning

The design of the proposed system requires positioning the VW inside the solid of Manipulability. This is the intersection of two solids, the bigger, the RW that spans the space where we can work on the other side the VW, which corresponds to the RW subsection we want to use.

This intersection affect zones with different values of μ (different colored volumes $v_i$ in figure 1). The use of this concept has the difficulty of finding the best relative positioning, i.e. what is the best area of RW for that size of VW, and for the application which we will do in this virtual environment

We modify the previously used global optimization algorithm for solving it. The main advantage obtained with the use of this modified algorithm compared to the previous, Simulated Annealing-SA [12], is that in the case of the use of SA the ability to converge sometimes was compromised if there was much difference between the size of RW and VW, so we could stay in local minima. Now the obtained search process is therefore more general.

### 4.1 Interference Factor-IF

Optimal navigation of a single device has been defined in previous work by the coefficient of Useful manipulability [13]. However, when the system consists of two devices, the behavior of one influences the other. While the two haptic devices do not perform a Dual Arm Cooperative Task Execution [14], there is interference because we have two haptics working in the same VW. We define Interference Factor (IF) as the index to quantify that effect. For its definition is necessary to study NFM tasks of each device, as well as introducing a time base. So taking into account not only how many times you visit a voxel of VW, but in what instant, and the proximity of the voxels that both Haptics visit in the same moment.

Additionally we must consider that there is a task, in this case the tool's operation, which can be primary. In this case we can think about minimizing the interference factor of the camera on the tool, providing NFM modification of the OMNi camera, looking for a new optimal path.

## 5 Results

In Insight ARTHRO VR, containing two devices, the application is centered on a virtual model of the human shoulder. We compare the optimal XYZ relative positioning for a set of different operations. We obtain these optimal positioning and the $\hat{\mu}_v$ values corrected with the new IF index.

Interference factor is calculated considering a time base. To do this, when we create the NFM, is incorporated in each voxel, not only the value of visits to this voxel, but also the instant of time of each visit. So when we study the comparison of dual work with two haptic devices, we must consider where to find the End Effector (EE) of each device at all times.

The IF is a function of the distance between the EE of each device so that if the distance is reduced, should be incorporated a real interference in the devices movements, since the rate of Manipulability of individual haptic, is going to be conditioned by the movement of the other.

The IF is modeled as an exponential value and corresponding to a maximum value of 1, without interference from a distance that our case is 5 voxels. For the positioning based in Simulated Annealing + IF a cell for the size of VW of 2mm is selected. Then IF is effective in a distance of 10mm between both EE. Moreover, with this size of the grid we can simplify assuming $\mu_{v\ ijk} = \mu_{ijk}$ calculated by (1), that is, we can suppose in each cell the value of the index of Manipulability is constant, so (2) can be simplified to:

$$\hat{\mu}_v = \sum_{ijk} \mu_{ijk} \cdot f_{ijk} \tag{3}$$

We have to realize the study of a system that is going to involve two OMNi devices, provided that in case of study, an operation of minimally invasive surgery, they are going to play roles of video camera and operation tool. Therefore there have been defined the corresponding VW of VW-camera and VW-tool. In these VW both values of Navigation Frequency Map (NFM) (Figure 2) must be indicated. With this information we incorporate the value of time each voxel is visited and the instant of the visit.

Once obtained the maps of frequencies for each of two devices there begins the process of search of the ideal positioning. The initial parameters of the Simulated Annealing [15] are:

Initial Error: error_i = 0.12
Initial Probability: pr_i = 0.28
Initial Temperature: $temp\_i = \frac{-error\_i}{\log(pr\_i)} = 0.125$

The "condition of cooling " is temp=temp*0.92. The process will continue while the condition is fulfilled of temp > 0.005.

The initial placement of the VW must be arbitrary in order to avoid local minima. As the temperature is modified, jumps of position are going to be realized, and we have introduced too a bigger jumps in this version. In every temperature the variation of position for each of the directions XYZ is calculated by the formulae:

$$\partial x = \frac{k}{6.5} \cdot random \cdot \frac{temp}{temp\_i} \cdot \quad \partial y = \frac{k}{6.5} \cdot random \cdot \frac{temp}{temp\_i} \cdot \quad \partial z = \frac{k}{6.5} \cdot random \cdot \frac{temp}{temp\_i} \cdot$$

where:

k is a constant proportional to the resolution of the grid
random is a random Lumber between 0 and 1.

The conditions of acceptance are one of the following:

$$\hat{\mu}_{\text{v}} > \hat{\mu}_{\text{v-accepted}} \quad p_r > p_a \, .$$

being:

$$p_r = \exp\left( -\frac{\hat{\mu}_{\text{v-accepted}} - \hat{\mu}_{\text{v}}}{temp} \right)$$

pr – value of the probability at a temperature:
pa – a random number between 0 and 1.

If this positioning is accepted, this cell turns into the new ideal point to place the VW:

$$\hat{\mu}_{\text{v-accepted}} = \hat{\mu}_{\text{v}}$$

However, in each case, before considering the value $\hat{\mu}_{\text{v-accepted}}$ is necessary to check whether there have been problems of interference with this configuration. IF factor is a characteristic of the operation being simulated, so there are interventions within the same virtual environment, where interference will occur and other interventions that do not.

Thus, the optimal solution for each of two devices OMNi will come indicated by the position XYZ that corresponds to this ideal value of convergence. The results indicate the position XYZ where the optimal performance for the OMNi is obtained from the coordinate origin at the center of OMNi device, and the corresponding value of $\hat{\mu}_v$.

### 5.1 Different Virtual Scenarios

In order to study the effect of modifying NFM with the same haptic device in the same virtual environment, we selected additional surgeries techniques:

**Surgery for shoulder instability.** The Bankart lesion is a tear on the labrum in the lower part of the shoulder joint [16]. A SLAP lesion involves the labrum and the ligament on the top part of the shoulder joint [17]. The first operation was a shoulder arthroscopy where most part of the work is made in the border of the glenohumeral zone. The problem to solve is called **Bankart lesion**, and the intervention consists of several steps: Bankart's injury is opened with arthroscopic instrumentation to obtain osseous bleeding tissue. After this, mini-screws have to be placed at the edge of the glenoid cavity and threads of suture across the labrum and from the glenohumeral ligaments. Then the ligaments and the labrum must be knotted and prefixed to the edge of the glenoid cavity. Finally the opening is closed. According to the analysis of the movements of the surgeon in this type of intervention, we created a NFM (Figure 3-1). The **SLAP lesion** involves the work in the top part of the joint, so both of them Bankart and SLAP are located in the shoulder joint but on the bottom or in the top. For SLAP lesion we created a NFM (Figure 3-2).

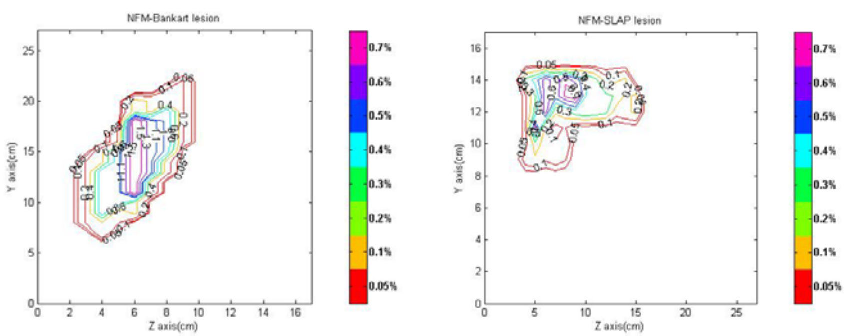


**Fig. 3**. 3-1. Frequency map corresponding with the Bankart lesion. 3-2. Frequency map corresponding with the SLAP lesion.

**Surgery for impingement syndrome.** Damaged or inflamed tissue is cleaned out in the area above the shoulder joint itself. The surgeon may also cut a specific ligament and shave off the under part of a bone. This under part of the bone is called the acromion. Removing a part of the acromion can stop the tendons of the rotator cuff from rubbing on the bone. This type of surgery is called an **Acromioplasty** [18]. So, in this intervention, most part of the work is done in the surroundings of the acromion. For Acromioplasty we created a NFM (Figure 4).

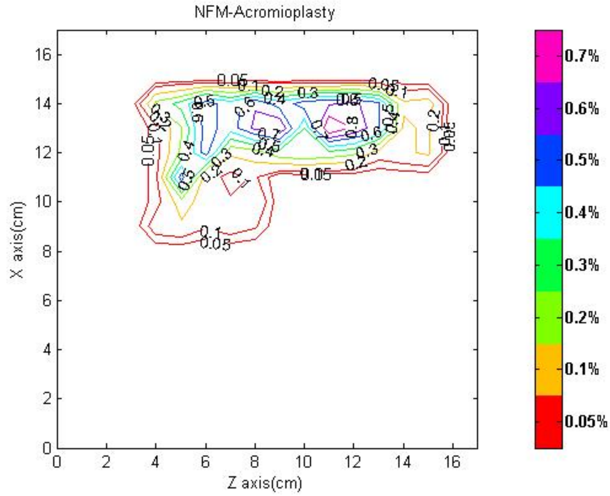


**Fig. 4.** Frequency map corresponding with Acromioplasty

**Rotator cuff disorders.** These are irritations in or damage to tendons around the shoulder. The selected operation is called Bursectomy. It is a shoulder arthroscopy where most part of the work is made in the subacromial area. The subacromial bursa is a tissue that serves as shock absorber and that diminish the rubbing between the acromion and the supraspinous ligament [19]. The patient with problems of the muff has an inflammation and hypertrophy of the bursa, called bursitis. The Bursectomy consists of drying out up the inflamed bursa. See the corresponding NFM in Figure 5.

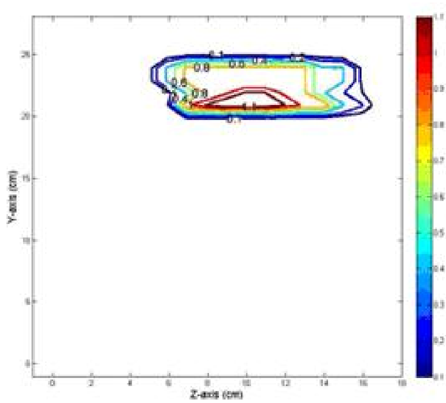

**Fig. 5.** Frequency map corresponding with Bursectomy

The results obtained by high resolution whole-exploration including IF factor, for optimal position XYZ are:

Bankart lesion:

OMNi-tool: $\hat{\mu}_V$ = 0.9176, position (-41, 139, 252) millimeters.

OMNi-camera: $\hat{\mu}_V$ =0.897, position (-10, 112, 109) millimeters.

SLAP lesion:

OMNi-tool: $\hat{\mu}_V$ = 0.9384, position (-38, 167, 263) millimeters.

OMNi-camera: $\hat{\mu}_V$ =0.897, position (-9, 98, 113) millimeters.

Acromioplasty:

OMNi-tool: $\hat{\mu}_V$ = 0.9384, position (-40, 143, 234) millimeters.

OMNi-camera: $\hat{\mu}_V$ =0.897, position (-10, 107, 101) millimeters.

Bursectomy operation:

OMNi-tool $\hat{\mu}_V$ = 0.908, position (51, 139, 250) millimeters.

OMNi-camera: $\hat{\mu}_V$ =0.897, position (-14, 115, 121) millimeters.

**Acknowledgments.** I would like to thank the anonymous reviewers for their helpful comments, Gracian Trivino and the rest of the GMRV group at URJC. This work has been partially funded by the Spanish Ministry of Education and Science IN2007-67188 and Cajal Blue Brain project.

## References

1. Yoshikawa, T.: Manipulability and redundancy control of robotic mechanisms. In: Proceedings of IEEE International Conference on Robotics and Automation, vol. 2, pp. 1004–1009 (March 1985)
2. Agha, R., Muir, G.: Does laparoscopic surgery spell the end of the open surgeon? J. R. Soc. Med. 96, 544–546 (2003)
3. Ahlberg, G., Heikkinen, T., Iselius, L., Leijonmarck, C.-E., Rutqvist, J., Arvidsson, D.: Does training in a virtual reality simulator improve surgical performance? Surg. Endosc. 16, 126–129 (2002)
4. Moore, M.J., Bennett, C.L.: The Learning Curve for Laparoscopic Cholecystectomy. The American Journal of Surgery 170(1), 55–59(5) (1995)
5. Yokokohji, Y., San Martin, J., Fujiwara, M.: Dynamic Manipulability of Multifingered Grasping. IEEE Transactions on Robotics 25(4), 947–954 (2009)
6. Gallina, P., Rosati, G.: Manipulability of a planar wire driven haptic device. Mechanism and Machine Theory 37(2), 215–228 (2002)
7. Cho, C., Kim, M., Song, J.: Direct Control of a Passive Haptic Based on Passive Force Manipulability Ellipsoid Analysis. International Journal of Control, Automation, and Systems 2(2), 238–246 (2004)
8. Murray, R.M., Li, Z., Sastry, S.S.: A mathematical introduction to robotic manipulation. CRC Press, Inc., Boca Raton (1994)

9. Yamamoto, Y., Yun, X.: Unified analysis on mobility and manipulability of mobile manipulators. In: Proceedings. 1999 IEEE International Conference on Robotics and Automation, Detroit, vol. 2, pp. 1200–1206 (1999)
10. Yokokohji, Y., Yoshikawa, T.: Guide of master arms considering operator dynamics. Journal of dynamic systems, measurement, and control 115(2A), 253–260 (1993)
11. Cavusoglu, M.C., Feygin, D., Tendick, F.: A Critical Study of the Mechanical and Electrical Properties of the PHANToM Haptic Interface and Improvements for High Performance Control. Teleoperators and Virtual Environments 11(6), 555–568 (2002)
12. Weise, T.: Global Optimization Algorithms. Theory and Application. Online e-book under GNU Free Documentation License (2009), `http://www.it-weise.de/projects/book.pdf`
13. San Martin, J., Trivino, G.: Mechanical design of a minimal invasive surgery trainer using the manipulability as measure of optimization. In: Proc. IEEE Int. Conf. Mechatronics (ICM), Kumamoto, Japan, pp. 1–5 (May 2007)
14. Lee, S., Lee, J.M.: Task-oriented dual-arm manipulability and its application to configuration optimization. In: Proceedings of the 27th IEEE Conference on Decision and Control 1998, December 7-9, pp. 2253–2260 (1988)
15. Aragon, C.R., Johnson, D.S., McGeoch, L.A., Shevon, C.: Optimization by Simulated Annealing: An Experimental Evaluation Part II, Graph Coloring and Number Partitioning. In: Operations Research, vol. 39(3), pp. 378–406 (1991)
16. Phillips, B.B.: Arthroscopy of the upper extremity. In: Canale, S.T., Beatty, J.H. (eds.) Campbell's Operative Orthopaedics, 11th edn., ch.49. Mosby Elsevier, Philadelphia (2007)
17. Snyder, S.J., Karzel, R.P., Pizzo, W.D., Ferkel, R.D., Friedman, M.J.: SLAP lesions of the shoulder. Arthroscopy: The Journal of Arthroscopic & Related Surgery 6(4), 274–279 (1990) ISSN 0749-8063
18. Beasley Vidal, L.S., et al.: Shoulder injuries. In: McMahon, P.J. (ed.) Current Diagnosis and Treatment in Sports Medicine, pp. 118–145. McGraw-Hill, New York (2007)
19. Phillips, B.B.: Recurrent dislocations. In: Canale, S.T., Beatty, J.H. (eds.) Campbell's Operative Orthopaedics, 11th edn., ch. 45. Mosby Elsevier, Philadelphia (2007)